

ly available, there is no evidence of this reaction taking place when the second reduction product is formed on the electrode surface. Instead, its formation results in a poisoning of the display electrode, and accounts for the "fatigue" reported for displays which have undergone numerous cyclings, whereby "erasing" becomes increasingly more difficult.<sup>7</sup> This consequently renders the diheptyl viologen dibromide system unsuitable for long-life display applications.

\*Present address: Energy Research Labs, Department of Energies Mines Research, Ottawa, Ontario, Canada.

<sup>1</sup>C. J. Schoot, J. J. Ponjee, H. T. van Dam, R. A. van Doorn, and P. T. Bolwijn, *Appl. Phys. Lett.* **23**, 64 (1973).  
<sup>2</sup>I. F. Chang, B. L. Gilbert, and T. I. Sun, *J. Electrochem. Soc.* **122**, 955 (1975).  
<sup>3</sup>H. T. van Dam and J. J. Ponjee, *J. Electrochem. Soc.* **121**, 1555 (1974).  
<sup>4</sup>C. J. Schott, J. J. Ponjee, H. T. van Dam, R. A. van Doorn, P. T. Bolwijn, and S. van Houten, *SID Int. Symp.* p. 146 (1973).  
<sup>5</sup>W. M. Schwarz and I. Shain, *Anal. Chem.* **35**, 1770 (1963).  
<sup>6</sup>R. M. Eloffson and R. L. Edsberg, *Can. J. Chem.* **35**, 646 (1957).  
<sup>7</sup>*New Electronics* **8**, No. 18 (1975).

## Low-threshold room-temperature embedded heterostructure lasers\*

C. P. Lee, I. Samid, A. Gover, and A. Yariv

California Institute of Technology, Pasadena, California 91125  
 (Received 4 June 1976)

Room-temperature embedded double-heterostructure injection lasers have been fabricated using selective liquid phase epitaxial growth. Threshold current densities as low as 1.5 kA/cm<sup>2</sup> have been achieved in lasers grown through stripe windows opened in epitaxial GaAlAs masks.

PACS numbers: 42.60.Jf, 78.45.+h, 78.60.Fi, 68.50.+j

We have recently reported on a new technique, "embedded heterostructure liquid phase epitaxy", for growing, through openings in masks, prismatic layered structures.<sup>1</sup>

The first demonstration of the technique was in a GaAs-GaAlAs system and the mask material was Al<sub>2</sub>O<sub>3</sub>. For (100) GaAs substrates, prisms grown through openings parallel to the (011) or (011) cleavage planes have {111} facets.<sup>1</sup> Prisms grown through stripe openings in the [001] orientation (45° to the cleavage planes) tend to form rectangular shapes with (010) faces.<sup>2,3</sup> Double-heterostructure stripe lasers produced by this technique in the [011] direction had room-temperature threshold of 5 kA/cm<sup>2</sup>.<sup>2</sup> One of the reasons for this

relatively high current was excessive leakage current bypassing the active region.

In what follows we describe lasers produced with GaAlAs masks, instead of the previous Al<sub>2</sub>O<sub>3</sub>. These lasers, in which the leakage current was largely eliminated, had a room-temperature threshold of 1.5 kA/cm<sup>2</sup>.

The layer sequence and the growth method are illustrated in Figure 1. Two layers, a 3-μm p-GaAs (Ge doped) and a 1.4-μm n-Ga<sub>0.4</sub>Al<sub>0.6</sub>As (Sn doped) are grown on top of a (100) n-type GaAs substrate as shown (layers M1, M2). A series of 25-μm-wide stripe win-

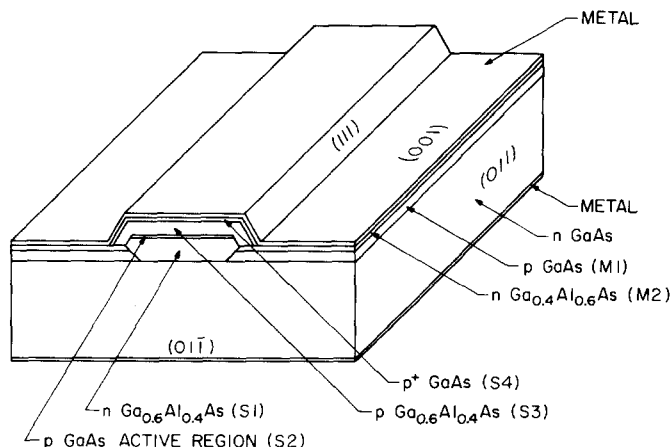


FIG. 1. Schematic drawing of an embedded heterostructure laser made with a GaAlAs-GaAs mask.



FIG. 2. Photomicrograph of the cross section of an embedded double-heterostructure laser grown through a window opened in a GaAlAs-GaAs mask.

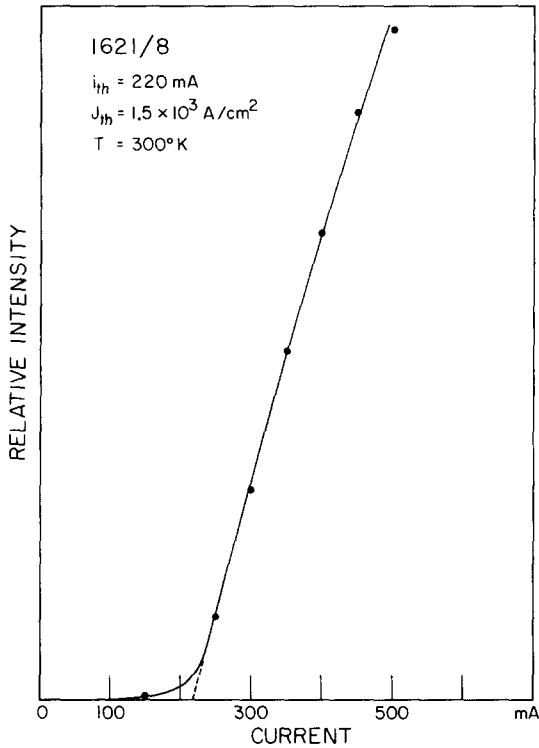


FIG. 3. Light intensity vs driving current of a typical laser.

dows are next opened in the layers using standard photolithographic techniques. The stripes were parallel to the  $[01\bar{1}]$  direction and an etching solution of  $H_2SO_4:H_2O_2:H_2O$  (5:1:1) was used to eliminate completely the epitaxially grown layers from the window areas so that the bottom of the etched channels consisted of the  $n$ -GaAs substrate.

In the second step a four-layer double heterostructure was grown through the channels. Except for a small overlay of the third and fourth layers, the growth was limited to the window areas. The layer composition is as follows: (S1)  $n$ -(Sn doped)  $Ga_{0.6}Al_{0.4}As$ , 7  $\mu m$  thick;

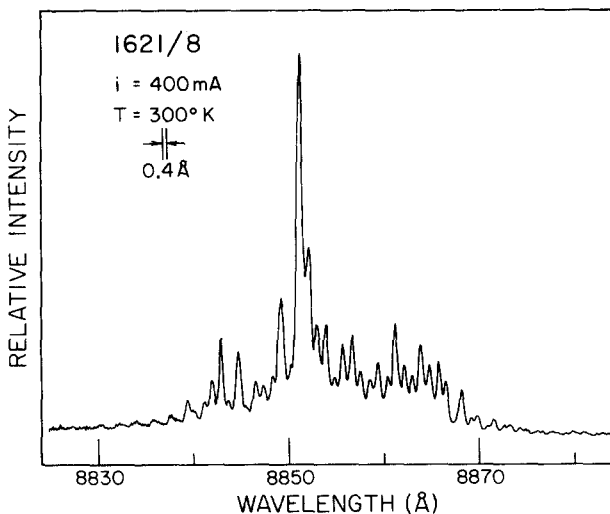


FIG. 4. Lasing spectrum of a pulse operated laser.

(S2)  $p$ -(Ge doped) GaAs, active layer  $\sim 0.2 \mu m$  thick; (S3)  $p$ -(Ge doped)  $Ga_{0.6}Al_{0.4}As$  layer, 8  $\mu m$  thick; (S4)  $p^+$ -(Ge doped) GaAs, contact layer 0.5  $\mu m$  thick. A photograph of the resulting structure is shown in Fig. 2. The growth temperature was near 800°C. A cooling rate of 0.1°C/min was used in growing the mask, while the DH laser structure was grown using a cooling rate of 0.05°C/min. The slower cooling rate in growing through the mask is necessitated by the faster growth rate in this case.<sup>1</sup>

Ohmic contacts were applied using evaporation of Cr-Au on the  $p$  side and Au-Sn electroless plating and alloying to the  $n$  side. The wafer was cleaved normal to the stripes' direction into bars 550  $\mu m$  wide to form the Fabry-Perot laser resonators, and separated into individual lasers by cleaving between the stripes. The individual lasers were mounted in indium-plated copper heat sinks.<sup>4</sup>

The reason for the layer sequence used in this laser can be understood by referring again to Fig. 1. Under forward biasing conditions of the laser in the stripe (positive voltage applied to the top contact) the junction ( $n$ - $Ga_{0.4}Al_{0.6}As$ - $p$ -GaAs) outside the stripe is reverse biased and conducts negligible current. Another bypass current path (i.e., current not injected into the active region) involves the forward biased  $p$ -GaAlAs- $n$ -GaAlAs junctions between layers S1 and S3 on either side of the active region. The junction barriers for this current are considerably larger than for the direct path. This electrical isolation forces the majority of the injection current to flow through the active region leading to low threshold current. The possible leakage path through the small-area interface between layers S1 and M2 was not effective in bypassing current, possibly because of poor electric contact between them and between the metal and the top GaAlAs layer M2, which is covered

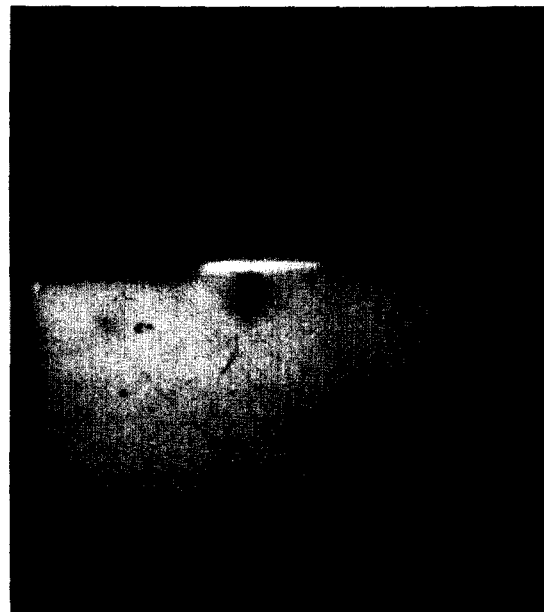


FIG. 5. Near-field radiation pattern of an embedded heterostructure laser.

by native oxide. The improved insulation of the GaAlAs mask was also evident from the absence of any light-emitting spots around the corners of the mesa and under the mask. Such spots, which are due to leakage current, were often seen in the  $\text{Al}_2\text{O}_3$  masked lasers.<sup>2</sup>

A plot of light intensity against current is shown in Fig. 3. Measurements were made with 100-nsec pulses at 500 Hz. The room-temperature threshold current density of  $1.5 \text{ kA/cm}^2$  is typical of most of the lasers. The oscillation spectrum is shown in Fig. 4 and was taken with 400-mA driving current which is almost twice the threshold value. Figure 5 shows a microphotograph of a laser radiation near-field pattern. The picture was taken through an optical microscope equipped with an image converter. The light intensity distribution along the active region is very uniform.

In summary, a modification of the embedded epitaxy technique which utilizes the native oxide of a GaAlAs layer allows for efficient electrical and optical confine-

ment, thus making possible low-threshold room-temperature embedded lasers.

The authors are grateful to Eric Mott for the fabrication of the laser heat sinks.

\*Work supported by the Office of Naval Research and by the National Science Foundation Optical Communication Program.

<sup>1</sup>I. Samid, C. P. Lee, A. Gover, and A. Yariv, *Appl. Phys. Lett.* **27**, 405 (1975).

<sup>2</sup>C. P. Lee, I. Samid, A. Gover, and A. Yariv, *Third American Conf. on Crystal Growth, Stanford, 1975* (unpublished); *Technical Digest of Topical Meeting on Integrated Optics, Salt Lake City, 1976, Paper WC6-1* (unpublished).

<sup>3</sup>D. W. Bellavance and J. C. Campbell, *Technical Digest of Topical Meeting on Integrated Optics, Salt Lake City, 1976, Paper PD8-1* (unpublished).

<sup>4</sup>J. C. Marinace, *IBM J. Res. Develop.* **8**, 543 (1964).

## Interferometric real-time display of cw dye laser wavelength with sub-Doppler accuracy

J. L. Hall\* and S. A. Lee

*Joint Institute for Laboratory Astrophysics, National Bureau of Standards and University of Colorado, Boulder, Colorado 80309*

(Received 7 June 1976)

We describe an automatic fringe-counting interferometer with real-time wavelength readout for cw laser sources. Sub-Doppler absolute wavelength accuracy ( $\sim 2 \times 10^{-7}$ ) is demonstrated with saturated absorption spectroscopy in neon.

PACS numbers: 42.60.Eb, 42.75.-r, 07.40.+a

The dye laser is bringing a new epoch in spectroscopy. Its tunability is of basic significance for fundamental precision measurements—for example, the spectroscopy of atomic hydrogen<sup>1</sup>—and for the investigation of new quantum systems for optical frequency standards.<sup>2</sup> For such studies the cw dye laser will be preferred to pulsed ones, in spite of the troublesome technology, because of its narrow spectral width and superior stability of amplitude and frequency. However, with the cw laser, one is faced with a very serious wavelength search problem. For example, typical cw dye lasers can continuously tune over at most a few Doppler absorption linewidths, but there are  $\approx 100$  such intervals per angstrom. In Doppler-free two-photon spectroscopy one is looking for weak narrow lines with no linear fluorescence signal at all. Thus it has been essential to develop the capability to rapidly readout a dye laser's wavelength with sub-Doppler absolute accuracy. We describe here an automatic-scanning corner-cube interferometer which provides about four independent measurements and display updates per second with a resolution of 120 MHz ( $\sim 0.004 \text{ cm}^{-1}$ ), about  $\frac{1}{10}$  of a typical Doppler linewidth. The update rate can be

decreased to obtain higher resolution. With improved optical components we expect that laser absolute wavelengths can be measured in 10 sec to  $< 10^{-8}$  (5 MHz, or 160 micro wave numbers).

An important contribution of our work is a resolution-enhancing concept which provides digital resolution of each optical fringe into 100 levels without a penalty in data acquisition time or bandwidth. The idea is that the fixed fringe rate generated by uniform translation of an interferometer reflector allows the fringe interrelations to be made with the metrology of frequency rather than distance.

In Fig. 1 we present a schematic of the interferometric and electronic systems which form our "lambda meter". Optically, it is a fringe-counting Michelson interferometer. With two folding mirrors, the carriage's motion shortens one arm and lengthens the other. The interferometer system counts the unknown wavelength in terms of the reference laser wavelength  $\lambda_{ref}$ . To eliminate optical feedback to the laser sources<sup>3</sup> and to keep the beams separate, we "stack" them into uncoupled sectors of the corner cubes. See Fig. 1. Care-